European Journal of Neuroscience, Vol. 12, pp. 4181–4194, 2000

Parkin expression in the adult mouse brain

Christine C. Stichel,[1,2] Martin Augustin,[2,*] Kati Kühn,[1] Xin-Ran Zhu,[1] Peter Engels,[2] Christoph Ullmer[2] and Hermann Lübbert[1,2]
[1]Department of Animal Physiology, ND5/132, Ruhr-University of Bochum, D-44780 Bochum, Germany
[2]Biofrontera Pharmaceuticals, D-51377 Leverkusen, Germany

Keywords: gene expression, neurodegenerative disease, Parkinson's disease, substantia nigra

Abstract

Mutations in a protein designated Parkin were shown to be involved in the pathogenesis of autosomal recessive juvenile parkinsonism. Nothing is known about its regional and subcellular distribution in the mouse. In order to elucidate the Parkin mRNA and protein distribution in the adult mouse, the mouse cDNA was cloned and polyclonal antisera were generated against the N-terminal part of mouse Parkin. The antibodies were shown to be specific using Western blot analysis, immunostaining of cells transfected with mouse Parkin and pre-absorption tests. The Parkin protein expression profile was studied using immunohistochemistry and Western blot analysis and was compared with that of the mRNA yielded by *in situ* hybridization and RT-PCR analysis. Parkin protein was widely distributed in all subdivisions of the mouse brain. Low levels were found in the telencephalon and diencephalon, while the brainstem contained a large number of cells heavily expressing Parkin. Ultrastructural analysis and double immunohistochemistry revealed that the majority of Parkin-expressing cells were neurons, while only single glial cells exhibited immunostaining. The protein was distributed nonhomogeneously throughout the entire cytoplasm. A subpopulation of Parkin-immunopositive cells displayed speckled immunodeposits in the nucleus. Dopaminergic cells of the substantia nigra pars compacta exhibited high levels of Parkin mRNA but no Parkin protein, while the striatum contained immunopositive profiles but no mRNA signals. Our data indicate that Parkin is neither restricted to a single functional system nor associated with a particular transmitter system. The speckled nuclear distribution of Parkin immunoreactivity strongly suggests a role for Parkin in gene expression.

Introduction

Human Parkin is a protein of 465 amino acids with a ubiquitin-like domain at the N-terminus and a ring-finger motif at the C-terminus (Kitada *et al*., 1998). Presumably, it possesses several phosphorylation sites and one putative N-myristoylation site (Abbas *et al*., 1999). The corresponding gene spans more than 500 kbp, has 12 exons and maps to chromosome 6q25.2–27 (Matsumine *et al*., 1997), a region of conserved synteny to mouse chromosome 17.

Recent studies suggest that Parkin contributes to the pathophysiology of Parkinson's disease. In patients with autosomal recessive juvenile parkinsonism, several microdeletions and point mutations have been identified in the Parkin gene (Hattori *et al*., 1998; Lücking *et al*., 1998; Tassin *et al*., 1998; Abbas *et al*., 1999; Nisipeanu *et al*., 1999). Additionally, Ser/Asn heterozygosity at codon 167 in the Parkin gene might represent a genetic risk factor for the development of sporadic Parkinson's disease (Satoh & Kuroda, 1999). Despite this considerable progress in linking Parkin mutations to Parkinson's disease, it remains unclear how these mutations induce the selective degeneration of dopaminergic substantia nigra neurons in Parkinson's disease. Based on protein structure analysis, a plethora of speculations about the function of Parkin has accumulated. Due to its structural similarity to the ubiquitin family members, it has been speculated that Parkin may interfere with the ubiquitin-mediated proteolytic pathway (Kitada *et al*., 1998). Furthermore, it was suggested that Parkin possesses DNA-binding and transcriptional activities, due to its in-between-ring-figures domain (Morett & Bork, 1999) or may play a role as a carrier protein in the vesicular transport system (Shimura *et al*., 1999).

One approach which may shed light on the role of Parkin in neuronal physiology is a comprehensive analysis of its expression pattern in the brain. To date, there are only short reports about Parkin expression in human (Kitada *et al*., 1998; Shimura *et al*., 1999; Solano *et al*., 2000), rat (Horowitz *et al*., 1999; D'Agata *et al*., 2000) and mouse central nervous system (CNS) (Kitada *et al*., 2000). Three of them concentrate on the distribution of Parkin mRNA (Kitada *et al*., 1998; D'Agata *et al*., 2000; Solano *et al*., 2000), while the others document the expression of the protein in a few selected brain regions (Horowitz *et al*., 1999; Shimura *et al*., 1999) and the study in the mouse showed only Northern blot analysis (Kitada *et al*., 2000).

In order to gain further insight into the role of Parkin in normal and Parkinson's disease physiology, we cloned murine Parkin cDNA and performed a detailed analysis of Parkin expression in the entire adult mouse brain. Since antisera from commercial sources showed no cross-reactivity with mouse Parkin, we generated specific polyclonal antisera against synthetic mouse Parkin peptides. With these antisera we performed immunoblotting and analysed the regional and subcellular expression patterns of Parkin protein in the adult mouse brain using immunohistochemistry. Furthermore, *in situ* hybridization and RT-PCR analysis were carried out to study the distribution pattern of Parkin mRNA.

Correspondence: Dr Christine C. Stichel, as above.
E-mail: christine.stichel-gunkel@ruhr-uni-bochum.de

**Present address*: Ingenium AG, D-82152 Martinsried, Germany

Received 3 April 2000, revised 22 August 2000, accepted 18 September 2000

Materials and methods

CDNA clones

For the isolation of murine Parkin cDNA, 2.4×10^6 clones of a murine brain cDNA library and 2.7×10^6 clones of a kidney cDNA library (both Edge BioSystems, Gaithersbürg, MD, USA) were screened with probes deduced from exon 2 of human Parkin. The nucleotide sequence of murine Parkin cDNA clones have been deposited in the GenBank nucleotide sequence database under the accession numbers (AF250293AF250295).

α-synuclein was cloned directly from murine whole-brain cDNA in both orientations into pCR2.1 (Invitrogen, The Netherlands) by PCR with primers msyn 2, 5′-GCAGAGGGACTCAGTGTGGTG-3′ and msyn 3, 5′-TTAGGCTTCAGGCTCATAGTCTTGGTA-3, corresponding to base pairs 19–459 of murine alpha-synuclein (ACC AF044672). A HindIII/NotI fragment containing the α-synuclein ORF in sense orientation was subcloned into the HindIII/NotI site of the episomal expression vector pEAK8 (Edge BioSystems).

Tissue collection

Experiments were conducted on C57BL/6 mice and Wistar rats of both sexes. All animal procedures were approved by local animal usage committees. The animals were housed in a 12 : 12 h light:dark cycle with free access to food and water.

Human brain tissue from four male individuals (mean age: 71 ± 6 years) was obtained from the Klinikum Leverkusen (Leverkusen, Germany). No cases had a history of neurological or psychiatric diseases. Specimens were autopsied within 24 h of death and the whole brains were stored in 4% paraformaldehyde (PA) at 4 °C until analysis.

Tissue preparation

Wild-type mice (C57BL/6) at postnatal age 2–3 months and Wistar rats at 3 months postnatal were killed by an overdose of a mixture of ketamine (100 mg/kg; Upjohn GmbH, Germany) and rompun (5 mg/kg; Bayer Leverkusen, Germany). Animals were transcardially perfused with phosphate-buffered saline (PBS) followed by one of the following fixatives: 4% PA in 0.1 M phosphate buffer (PB), 4% PA plus 0.1% glutaraldehyde in PB or periodate/lysine/2% paraformaldehyde (PLP) (McLean & Nakane, 1974) and a postfixation time of 4–48 h at 4 °C. Two animals were killed and stored at 4 °C for 24 h before fixation. After fixation animal and human tissues were (i) cryoprotected in 30% sterile, phosphate-buffered sucrose and frozen in methylbutan between –50 and –70 °C; (ii) embedded in paraffin, or (iii) processed for electron microscopy. For light microscopic immunohistochemistry, serial cryostat (20 μm) or paraffin (4 or 7 μm) sections were cut and mounted on Superfrost slides (Roth, Germany). Free-floating vibratome (50 μm) sections were used for electron microscopic analysis and 30 μm sagittal cryostat sections were processed free floating for *in situ* hybridization.

Antibody preparation

Polyclonal antibodies were raised in rabbits against synthetic peptides corresponding to residues 71–91 (QRPRRRSHETNASGGDEPQSTS; msParkin1) and residues 124–140 (DTDSKRDSEAARGPVK; msParkin2)of predicted murine Parkin. These regions were chosen because of their relatively high sequence heterogeneity to human Parkin protein. The peptides were coupled to keyhole limpet haemocyanin (KLH) before immunization. Three rabbits were injected subcutaneously with 500 μg of msParkin (Rb1 and Rb2 with msParkin1, Rb3 with msParkin2) emulsified in Freund's complete adjuvant, and then boosted nine times with either 500 or 250 μg of the peptide in Freund's incomplete adjuvant. Animals were bled 160 days (Rb1 and Rb2) or 108 days (Rb3) after the first immunization and the crude antisera were used for the following studies. The antisera raised to msParkin1 were named Rb1-antimsParkin1 or Rb2-antimsParkin1, while the antiserum raised against msParkin2 was named Rb3-antimsParkin2.

Protein extraction and immunoblots

For immunoblotting total mouse brain, dissected mouse brain regions or transfected cells were homogenized in triple detergent lysis buffer (50 mM HEPES [pH 7.4], 150 mM NaCl, 10 mM EDTA, 1% NP40) containing complete protease inhibitor cocktail (Boehringer Mannheim, Germany) using a Teflon/glass homogenizer at 4 °C. Homogenized samples were left on ice for 30 min and centrifuged at 14 000 r.p.m. 20 000 ***g*** in a precooled centrifuge. The supernatant was diluted 1 : 1 in 2x Laemmli sample buffer and boiled. Protein determination was performed by the method of (Neuhoff *et al*., 1979).

Proteins were electrophoretically separated on a 10% or 12% polyacrylamide gel containing sodium dodecyl sulphate (SDS), and transferred onto a nitrocellulose filter at 4 °C with 100 mA for 1 h. Blocking was performed with 3% milk powder, 2% bovine serum albumin (BSA) in TBS-Tween (0.1% Tween, 20 mM TBS) at room temperature (RT) for 1 h. Incubation with the primary antisera or the pre-immune sera was performed at 1 : 1000–1500 (Rb1-antimsParkin1 and Rb3-antimsParkin2) and 1 : 500 (Rb2-antimsParkin1), respectively, diluted in blocking buffer at RT, followed by washing in TBS-Tween and incubation in antirabbit HRP-coupled secondary antibody (1 : 4000 in 1% milk powder, 0.5% BSA in TBS-Tween; Amersham, Germany) at RT for 1.5 h. The blots were washed and developed using the ECL system (Amersham, Germany).

Transfections

Transfection of pEAK8 expression vectors containing complete open reading frames of murine Parkin or murine α-synuclein into COS and HEK cells was carried out with Lipofectamine Plus reagent (Life Technologies, Germany) according to the manufacturer's recommendations. Transfected cells were plated onto poly L-lysine (0.1 mg/mL, 24 h, 4 °C)-coated coverslips. Plated cells and cell extracts were used for examining the specificity of msParkin-antisera by immunocytochemistry, immunoblotting and *in situ* hybridization.

Immunohistochemistry

For single labelling, 4% PA-fixed transfected cells and frozen or deparaffinized sections were pre-incubated with 3% H_2O_2 (v/v) in methanol to block endogenous peroxidase (10 min at RT), followed by 3% normal goat serum in 0.01 M PBS (10 min at RT) to reduce nonspecific binding. Some sections were incubated in 0.4% Triton-X-100 (15 min at RT) to enhance penetration. Then the sections were reacted with either Rb1-/Rb2-antimsParkin1 or Rb3-antimsParkin2 diluted 1 : 4000–8000, sheep antirat tyrosine hydroxylase (TH, 1 : 500; Chemicon, Germany) (over night/4 °C) or mouse antimouse NeuN (1 : 500; Chemicon), followed by the appropriate biotinylated secondary antiserum (1 : 300 in 0.01 M PBS; 45 min at RT; Vector Laboratories, CA, USA) and the avidin-biotinylated peroxidase complex (1 : 200 in 0.01 M PBS; 45 min at RT, Vector Laboratories). Following these incubations, peroxidase enzyme activity was demonstrated by immersing the sections in a solution of 7% 3,3'diaminobenzidine tetrahydrochloride (DAB, Sigma, Germany) in 0.1 M PB containing 0.01% H_2O_2 for 5–10 min. For enhancement of the staining a silver intensification method was performed as described (Stichel *et al*., 1990).

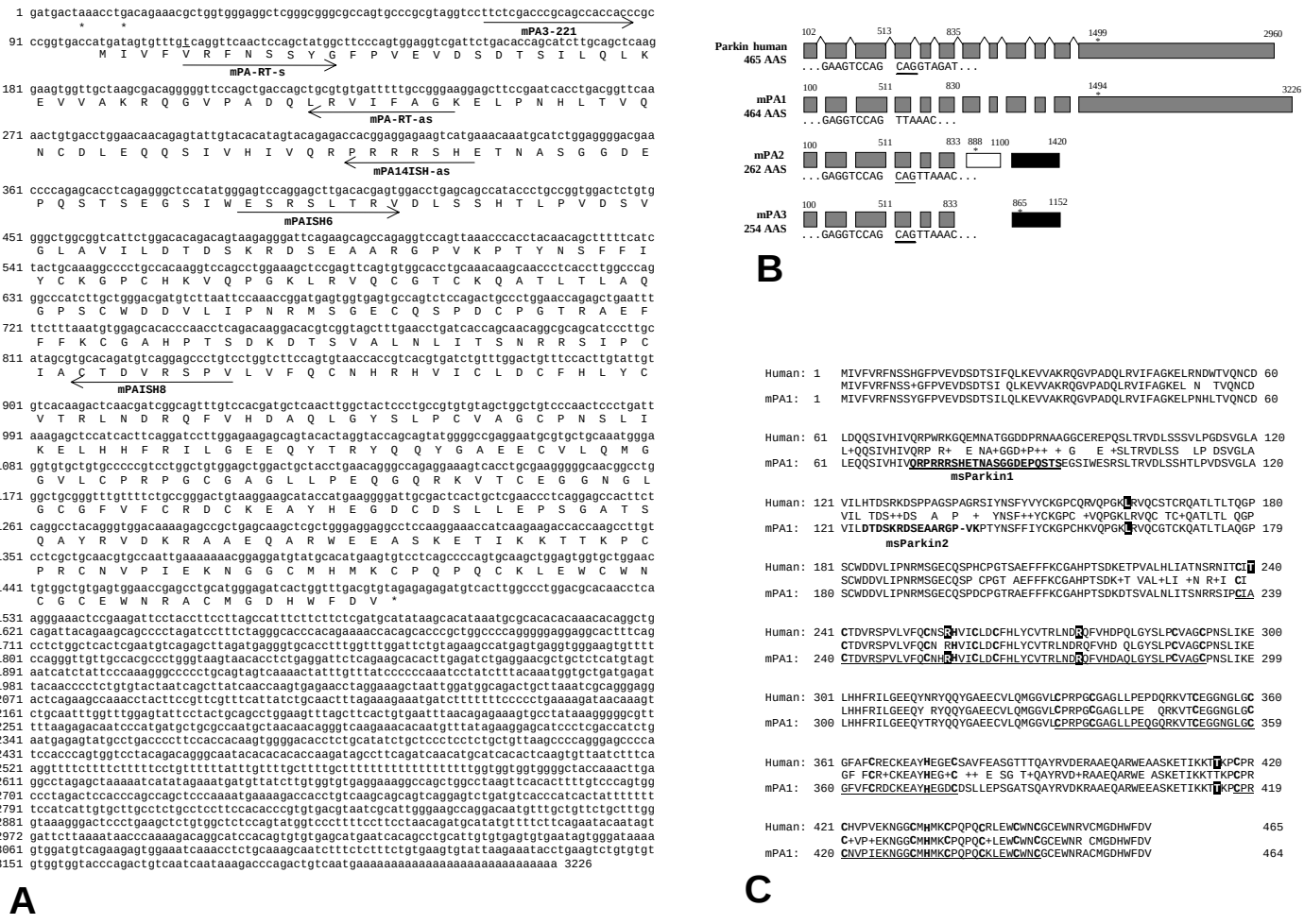

FIG. 1. (A) cDNA and protein sequence of murine Parkin; in-frame stop codons are indicated by asterisks, nucleotide positions of primers used for RT-PCR and generation of riboprobes are indicated by arrows. (B) Alignment of murine Parkin cDNA clones mPA1–mPA3 compared with human Parkin gene structure (cf. Kitada *et al*., 1998). Positions of exons (grey squares) are deduced from the human sequences. Numbers define nucleotide positions corresponding to sequences of mPA1–mPA3 as deposited in the Genbank database: mPA1, accession number AF250293; mPA2, accession number AF250294; mPA3, accession number AF250295. Numbers combined with asterisks indicate positions of stop codons. mPA1 contains an open reading frame of 1392 bp (nt 100–1492) encoding 464 amino acids, whereas mPA2 and mPA3 exhibited open reading frames of 262 and 254 amino acids, respectively. Due to alternative splicing, mPA1 lacks the first three nucleotides of presumed exon 4 (CAG, underlined) that exist in human Parkin (nt 514–516; accession number AB009973) and clones mPA2 and mPA3 (nt 512–514). Without this exception, the sequence of mPA2 and mPA3 was identical to mPA1 from nt 1–833, but was followed by an alternative 3′ sequence. Black boxes indicate identical sequences in alternative 3′ ends of mPA2 and mPA3. (C) Comparison of murine and human Parkin amino acid sequences with a consensus sequence given in between. Residues for which pathological mutations have been described in humans are highlighted. Underlined amino acids define the highly conserved C3HC4-type ring fingers and the C6HC IBR region with conserved cysteine and histidine residues indicated in bold. For the production of polyclonal antibodies, synthetic peptides corresponding to residues 71–91 (msParkin1) and residues 124–140 (msParkin2) were used.

For double labelling, deparaffinized sections were simultaneously incubated with primary Parkin antibodies and either sh anti-TH or ms anti-NeuN overnight at 4 °C, which were visualized with CY3-conjugated antirabbit IgG and biotinylated horse antimouse or biotinylated antisheep (1 : 300, Vector Laboratories) followed by avidin-FITC (1 : 500; Vector Laboratories). Sections were cover-slipped with Vectashield (Vector Laboratories). Cross-reactivity experiments were performed to ensure the specificity of the signals.

Specificity of the Parkin staining was confirmed by different sets of controls. First, we performed antigen absorption tests. For that purpose we pre-incubated the antisera with 4–10 mol of msParkin or an irrelevant peptide (ms α-synuclein aa117–131) overnight at 4 °C. In addition, some sections were incubated without primary antibodies or with the pre-immune serum to rule out false-positive results.

For pre-embedding electron microscopic immunohistochemistry, vibratome sections were processed in the same way as the sections for light microscopy. After DAB reaction the pontine nuclei, the striatum and the substantia nigra (SN) were dissected, washed in 0.1 M PB, post-fixed for 1 h in 2% OsO_4, dehydrated with graded concentrations of ethanol and propylene oxide and flat-embedded in Epon. Representative ultrathin sections were collected on Formvar-coated grids, contrasted with uranyl acetate and lead citrate.

Rt-PCR

Total cellular RNA from various brain regions of 8-week-old C57BL/6 mice was isolated with TRIZOL reagent (Life Technologies) according to the manufacturer's recommendations. To reduce contamination by genomic DNA, 20 µg RNA was

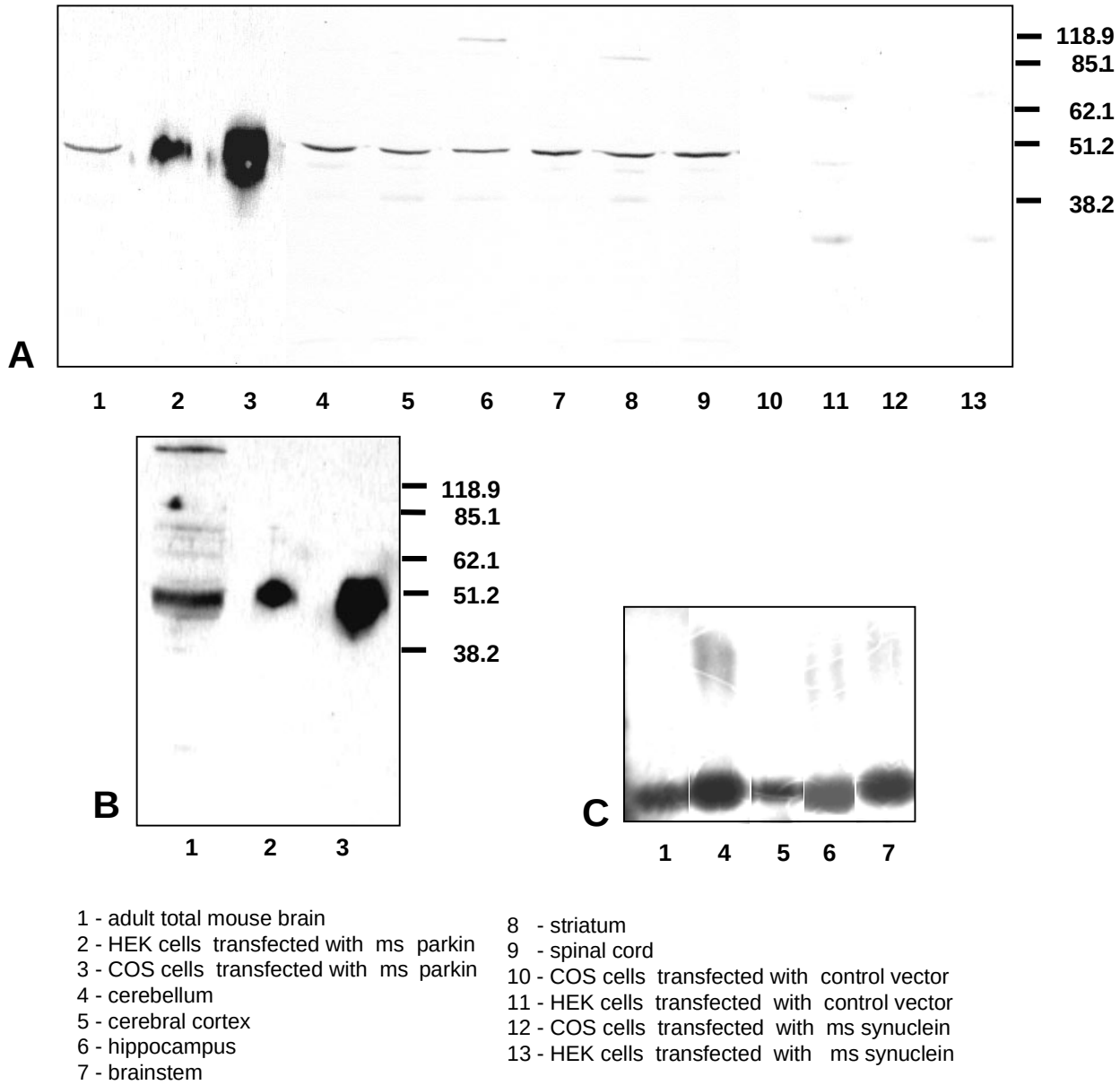

FIG. 2. Western blot (A and B) and RT-PCR (C) analysis of Parkin expression in various brain regions and transfected COS and HEK cells. Immunoblots with (A) Rb1-antimsParkin1 and (B) Rb2-antimsParkin1.

treated for 15 min at 37 °C with 10 U DNAse I (RNAse-free, Boehringer Mannheim), followed by phenol/chloroform extraction and ethanol precipitation.

Five micrograms of each total RNA was subjected to RT-PCR with an annealing temperature of 60 °C and 32 cycles after reverse transcription with hexanucleotide primers.

Primers used for the amplification of a 130-bp Parkin fragment were:

sense primer mPA-RT-s, 5′-TCAGGTTCAACTCCAGCTAT-GGC-3′; antisense primer mPA-RT-as, 5′-TCCCGGCAAAAATC-ACACGCAGC-3′ (Fig. 1a). PCR was carried out with 0.2 μCi ^{32}P-dCTP added to each reaction. Appropriate controls for the specificity

FIG. 3. Parkin protein distribution in the adult mouse brain, immunohistochemical staining with Rb1-antimsParkin1. (A and B) Low-power micrographs showing the overall distribution of Parkin-immunopositive cells in a cranial (A) and caudal section (B) of the brain, respectively. (C–G) Various regions of the mouse brain: C, retrosplenial cortex; D, brainstem; E, Substantia nigra; F, hippocampus, G, dorsal cochlear nucleus and H, striatum. (I) Neurons of the cerebral cortex displaying granular staining in the cytoplasma and processes. (K) Abolition of staining by prior absorption of the antibody with its specific peptide antigen in the dorsal cochlear nucleus. This section is adjacent to the section shown in G. Stars mark corresponding blood vessels. Abbreviations: 7, facial nucleus; APT, anterior pretectal nucleus; CA1, hippocampal field CA1; CA3, hippocampal field CA3; CPO; caudal periolivary nucleus; DG, dentate gyrus; IMLF, interstitial nucleus of the medial longitudinal fasciculus; Int, interposed cerebellar nucleus; Lat, lateral cerebellar nucleus; LPGi, lateral paragigantocellular nucleus; LSO, lateral superior olive; Med, medial cerebellar nucleus; ML, medial mammillary nucleus, lateral part; PCRt, parvicellular reticular nucleus; PnC, pontine reticular nucleus; R, red nucleus; S, subiculum; SC, superior colliculus; SNC, substantia nigra pars compacta; SNR, substantia nigra pars reticulata; VCP, ventral cochlear nucleus, posterior part. Scale bars, 100 μm (A–D and F), 50 μm (E, G, H and K) and 10 μm (I).

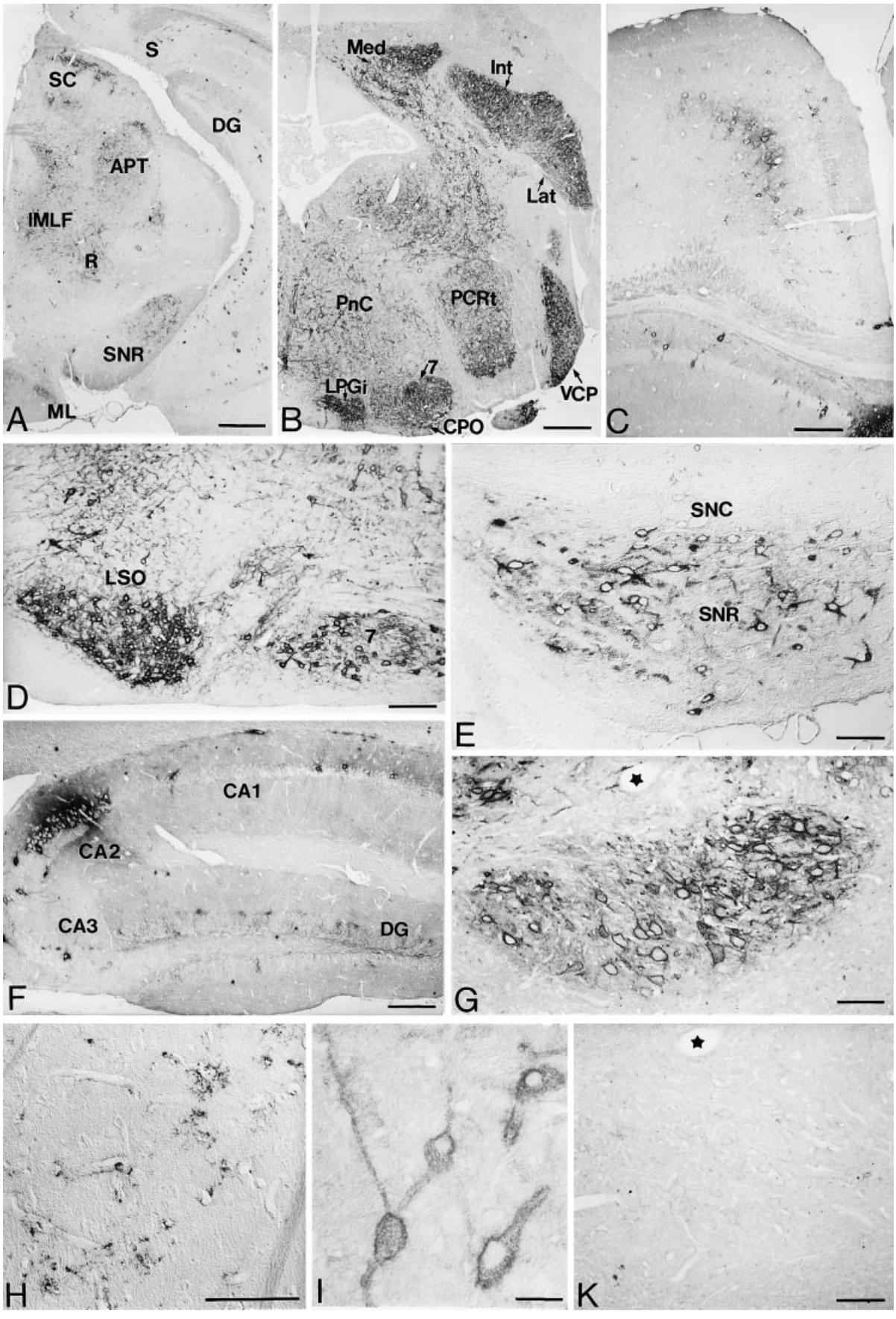
S
SC
DG
APT
IMLF
R
SNR
ML
A
Med
Int
Lat
PnC
PCRt
7
LPGi
VCP
CPO
B
C
LSO
7
D
SNC
SNR
E
CA1
CA2
CA3
DG
F
G
H
I
K

of the PCR reaction were performed with the following templates: Parkin cDNA clone mPA1, positive; RNA without reverse transcription, water, negative. After electrophoresis, 2.5% agarose gels were dried and exposed to X-ray films for 1 h.

Generation of riboprobes for in situ *hybridization*

Two different riboprobes were generated for *in situ* hybridization.

For riboprobe 1 a 268-bp fragment of murine Parkin was amplified by PCR with sense primers mPA3ISH-T7s, 5′-TTGTAATACGACTCACTATAGGGTTCTCGACCCGCAGCCACCACC-3′; mPA3–221, 5′ TTCTCGACCCGCAGCCACCACC-3′ and antisense primers mPA14ISH-T7as, 5′-TTGTAATACGACTCACTATAGGGTCATGACTTCTCCTCCGTGG-3′; mPA14ISH-as 5′-TCATGACTTCTCCTCCGTGG-3′ corresponding to bp 66–334 of the mouse Parkin cDNA sequence (Fig. 1A). Primers mPA3ISH-T7s and mPA14ISH-T7as contained the T7 promoter sequence. For generation of sense probes, mPA3ISH-T7s was combined with mPA14ISH-as, and for generation of antisense probes, mPA3–221 with mPA14ISH-T7as.

For riboprobe 2, a 448-bp fragment of murine Parkin was amplified by PCR with sense primers mPAISH5, 5′-TGTAATACGACTCACTATAGGGTGAGTCCAGGAGCTTGACACGAGT-3; mPAISH6, 5′-GAGTCCAGGAGCTTGACACGAGT-3′, and antisense primers mPAISH7, 5′-TTGTAATACGACTCACTATAGGGTACAGGGCTCCTGACATCTGTG-3′; mPAISH8, 5′-ACAGGGCTCCTGACATCTGTG-3′ corresponding to bp 391–839 of the mouse Parkin cDNA sequence (Fig. 1A). Primers mPAISH5 and mPAISH7 contained the T7 promoter sequence. For generation of sense probes, mPAISH5 was combined with mPAISH8, and for generation of antisense probes, mPAISH6 with mPAISH7.

Labelled mRNA probes were generated with T7 polymerase (Boehringer Mannheim) in the presence of digoxygenin (DIG)-labelled nucleotides.

The quality of the probes and the transcription efficiency was checked by Northern blotting and subsequent immunodetection using the anti-DIG antibody tagged with alkaline phosphatase (anti-DIG-AP; 1 : 2000; Boehringer Mannheim). The size of the probes was checked by agarose gel electrophoresis.

TABLE 1. Brain regions with Parkin immunoreactivity in neuronal somata

Brain region	Relative staining intensity
Telencephalon	
Neocortex	+
Retrosplenial cortex	++
Subiculum	+
Hippocampus proper	+++
Fascia dentata	+++
Amygdaloid nuclei	++
Induseum griseum	+++
Septum	++
Globus pallidus	+
Diencephalon	
Laterodorsal thalamic nucleus	++
Mammillary body	++
Zona incerta	++
Nucleus reticularis thalami	++
Mesencephalon	
Superior colliculus	++
Inferior colliculus	++
Red nucleus	+++
Praetectal nucleus	++
Substantia nigra (pars reticulata)	++
Oculomotor nucleus (III)	+++
Metencephalon	
Medial cerebellar nucleus (fastigial)	+++
Interposed cerebellar nucleus	+++
Lateral cerebellar nucleus (dentate)	+++
Myelencephalon	
Pontine nuclei	+++
Trigeminal nucleus (V)	+++
Abducens nucleus (VI)	+++
Facial nucleus (VII)	+++
Vestibular nucleus (VIII)	+++
Cochlear nucleus (VIII)	+++
Superior/inferior olive	+++
Periolivary nucleus	+++
Nuclei reticularis	++

Symbols represent semiquantitative evaluation of staining intensity: +, weak; ++, moderate, +++, strong.

In situ *hybridization*

The localization of Parkin mRNA by *in situ* hybridization (ISH) was performed in 4% PA-fixed, free-floating cryostate sections or 4% PA-fixed, transfected cells, as described by Wahle (1994). All incubations and washings were done in sterile 35-mm-diameter culture dishes and sections/coverslips with plated cells were handled with fine, autoclaved glass hooks. Brain sections and cells were prehybridized in hybridization buffer containing 50% formamide, 4x SSC (1x SSC = 0.15 M NaCl and 0.015 M sodium citrate, pH 7.0), 50 mM NaH_2PO_4 pH 6.5, 250 µg/mL denatured herring sperm DNA, 100 µg/mL tRNA, 5% dextransulphate and 1x Denhardt's solution. Hybridization was carried out overnight at 40 °C (for riboprobe 1)/ 50 °C (for riboprobe 2) with different concentrations of the RNA probes in hybridization buffer. After stringent washes at 45 °C (for riboprobe 1)/56 °C (for riboprobe 2) first in 2x SSC containing 50% formamide for 15 min, followed by 0.1x SSC containing 50% formamide for 15 min, 0.1x SSC for 30 min and a blocking step in 5% BSA in 0.1 M TBS, hybrid molecules were detected with sheep anti-DIG-AP antibody (1 : 2000) overnight at 4 °C and reacted with nitroblue tetrazolium (0.24 mg/mL, Sigma) and 5-bromo-4-chloro-3-indolyl phosphate (0.125 mg/mL, Sigma) in 0.1 M Tris, 0.1 M NaCl, 0.05 M $MgCl_2$ at pH 9.5. The reaction was stopped with 0.01 M Tris, 0.01 M EDTA pH 8.0.

Antisense and sense probes were used under identical conditions.

Data analysis

For histological identification of the nuclear boundaries, every tenth section was stained with cresyl violet. Brain sections were visualized at the microscopic level (Axioskop 2; Zeiss, Germany) under bright-

FIG. 4. Immunohistochemical staining of adjacent 4 µm-thick frontal paraffin sections with Rb1-antimsParkin1 (A, C and E) and anti-TH (B and D) or anti-NeuN antibodies (F). (A and B) Comparison of the distribution patterns of Parkin (A) and dopaminergic neurons (B) in sections through the mesencephalic region. (C and D) Parkin-immunopositive cells (C) do not colocalize with TH-immunopositive neurons in the SNC. Corresponding blood vessels are marked by asterisks. (E and F) Numerous Parkin-immunopositive cells express NeuN. Double-labelled cells are indicated by the same number. Asterisks mark the blood vessels. Abbreviations: R, red nucleus; SC, superior colliculus; SNC, substantia nigra pars compacta; SNR, substantia nigra pars reticulata; VTA, ventral tegmental area. Scale bars, 100 µm (A and B) and 10 µm (C–F).

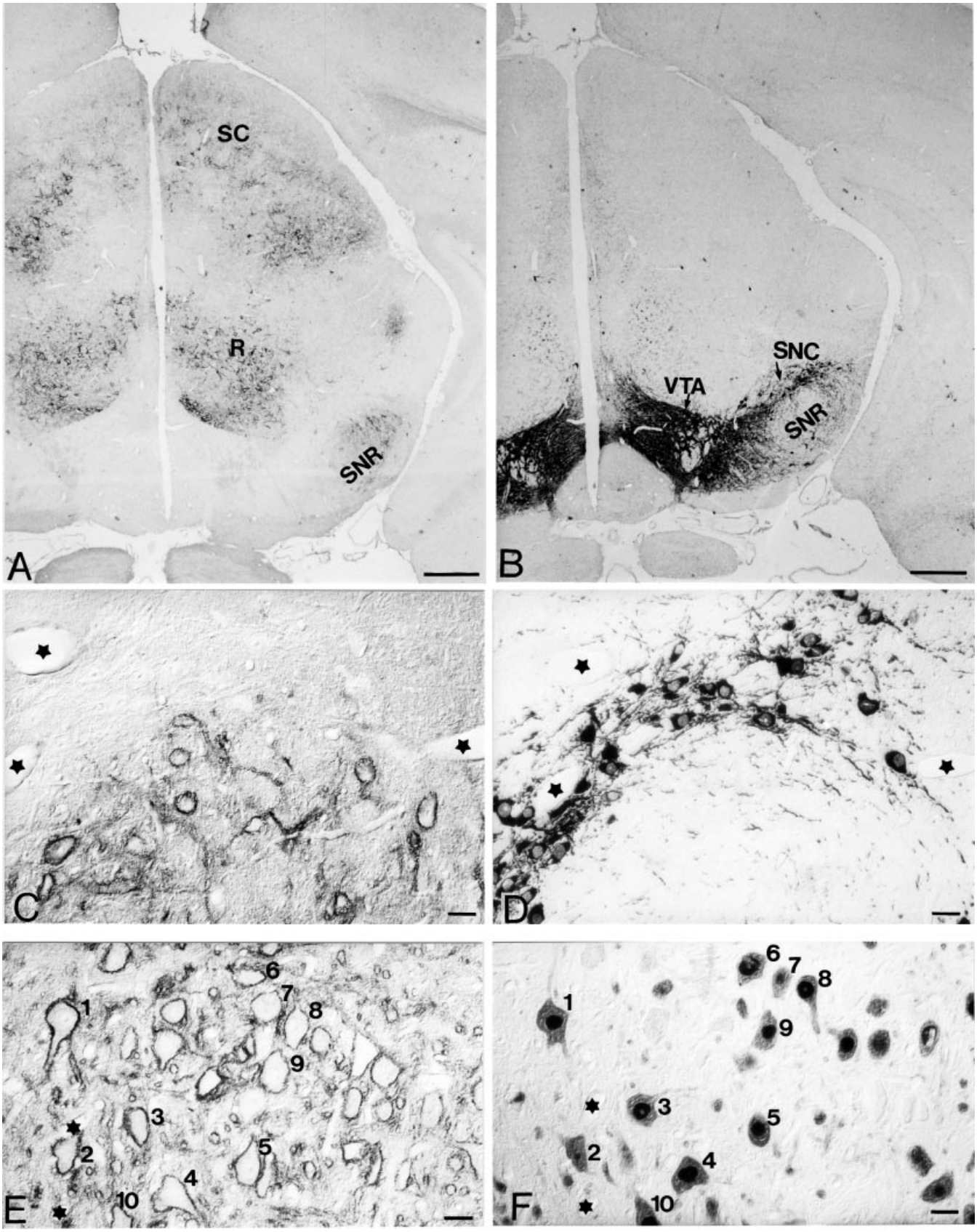
SC
R
SNR
A
SNC
VTA
SNR
B
C
D
6
7
8
1
9
3
2
5
4
10
E
6
7
8
1
9
3
5
2
4
10
F

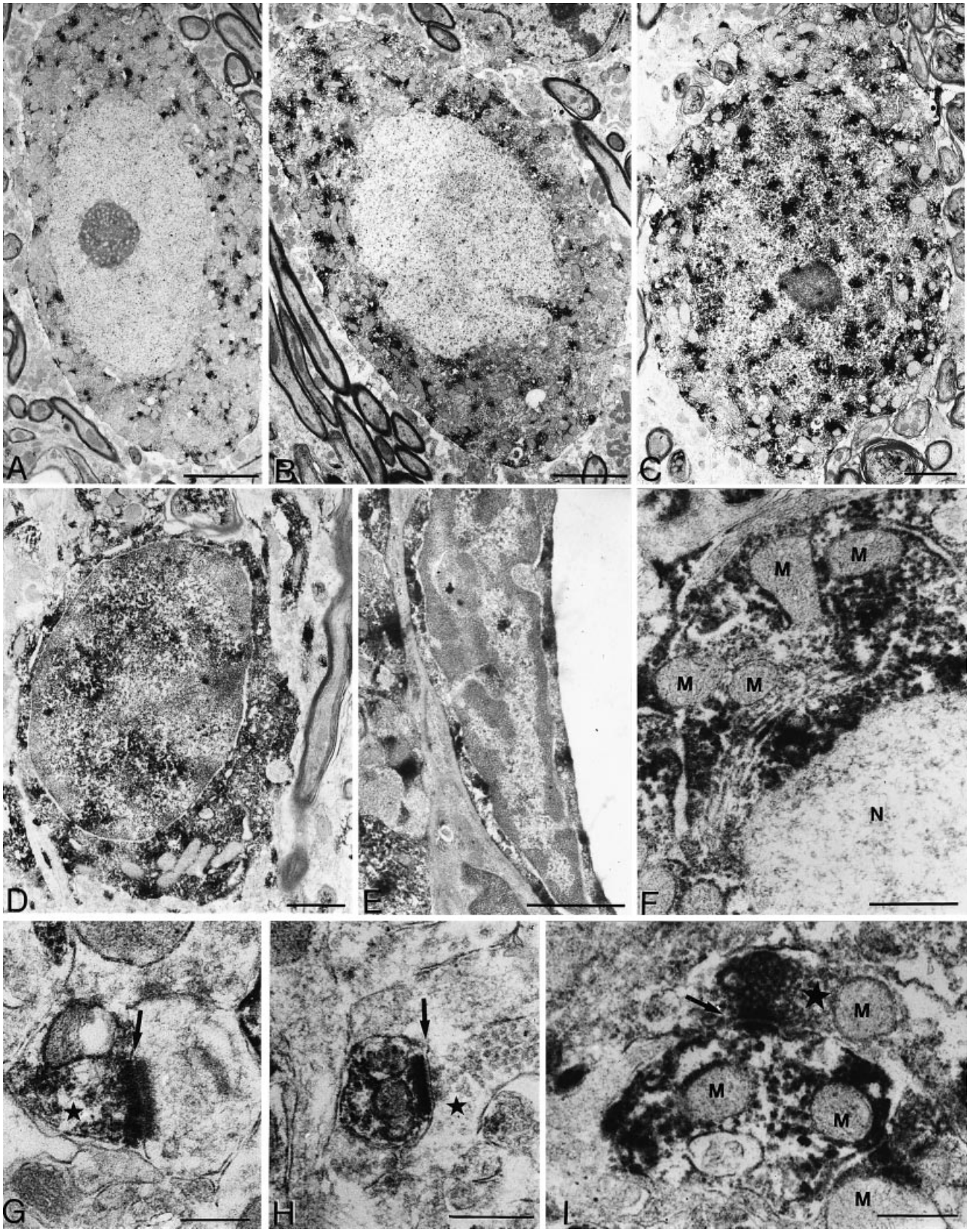
A
B
C
D
E
F
M
M
M
M
N
G
H
I
M
M
M
M

field illumination and Nomarski optics, or under epifluorescence. Structures were described according to the main subdivisions of the brain and were identified with the aid of atlases (Franklin & Paxinos, 1997; Paxinos & Watson, 1998). The anatomic terminology used in this study was based on these atlases. Photomicrographs were taken by using Agfapan APX 25 or Kodak Ektachrom P1600 films.

The staining intensity of the Parkin-immunoreactive neurons was semiquantitatively evaluated in the microscope. The staining intensities were rated into one of the following categories: (+), weak; (++) moderate and (+++), strong signal.

Ultrathin sections were photographed in a Zeiss 109 electron microscope using Kodak Technical Pan 120 films.

Results

Cloning of murine Parkin cDNAs

Two brain cDNA clones (mPA2, mPA4) and two kidney cDNA clones (mPA1, mPA3) were obtained which showed high sequence homology to human Parkin cDNA. Among these the clone (mPA1) isolated from murine kidney contained an insert of 3.2 kbp, encompassing an open reading frame of 1392 bp (Fig. 1A and B). The three other clones exhibited different sequences following exon 6 (mPA2, mPA3, Fig. 1B) and exon 3 (mPA4), respectively. Whereas mPA2 and mPA3 most probably represent alternatively spliced forms of murine Parkin (cf. Kitada *et al*., 2000), exon 3 sequences in mPA4 were followed by intronic sequences (not shown).

Sequence analysis of mPA1 revealed an open reading frame encoding 464 amino acids (Fig. 1A and C), the sequence of which is identical to that recently deposited by [14>]Kitada *et al*. (2000) in the GenBank database (accession number AB019558). In the protein encoded by mPA1, the presumptive start methionine is preceded by two in-frame translational stop codons (Fig. 1A). Comparison of the amino acid sequences of murine Parkin with that of human and rat Parkin proteins (accession number AF168004; D'Agata *et al*., 2000) shows an identity of 83% and 94%, respectively. This remarkable interspecies conservation is interrupted at amino acids 73–138, corresponding in part to exon 3 of human Parkin. In this region, the identity reaches only 56% between murine and human Parkin, but 84% between the murine and rat protein. Compared with the human protein, murine Parkin protein encoded by mPA1 lacks an alanine at amino acid position 138 (Fig. 1A and C), which exists in the amino acid sequences encoded by mPA2 and mPA3 (Fig. 1B). Within the two C3HC4 ring-finger domains and the IBR C6HC domain, all cysteine and histidine residues are conserved between all three species. Five mis-sense mutations have been described in human Parkin (Hattori *et al*., 1998; Abbas *et al*., 1999) which can be assumed as pathological mutations. Four of those amino acid positions Lys161, Arg256, Arg275 and Thr415 are conserved between mouse, rat and human Parkin. In contrast, instead of Thr240 an alanine is found in the mouse and rat sequences. This is noteworthy because it is assumed that the Thr240Arg might act as a pathological mutation by elimination of a presumed phosphorylation site for casein kinase II (Hattori *et al*., 1998), a site which does not exist in mouse and rat due to the presence of an alanine on amino acid position 240.

Parkin protein expression pattern

Specificity of the Parkin antisera

The specificity of our primary Parkin antisera and the immunohistochemical procedure was assessed by several criteria. (1) Using Western blot analysis, the antisera recognized the same pattern of bands with a major band of ≈50 kDa in the whole brain homogenates and a similar band in COS and HEK-cells transfected with the ms Parkin gene (Fig. 2A and B; Rb3-antimsParkin2, data not shown). The molecular weight of the major band corresponds to the expected size of ms Parkin. The much fainter bands detectable at about 40 and 85/118 kDa may represent either post-translational modifications of the protein (Horowitz *et al*., 1999) and/or truncated forms, encoded by the splicing variants (as discussed earlier) (Kitada *et al*., 2000). Western blots stained with the pre-immune sera were negative. The labelling of the 50 kDa band was therefore judged to be specific. (2) In immunohistochemistry, all antisera labelled the same cellular profiles in mouse and rat brains and stained strongly COS cells transfected with mouse Parkin. (3) Staining distribution was consistent from one brain to another and independent from the fixative chosen. (4) Immunolabelling in all brain regions investigated was abolished after pre-absorption of the polyclonal antibodies with the corresponding peptide msParkin (Fig. 3K). (5) No staining was observed when the primary antisera were replaced by the pre-immune sera or the primary and secondary antibodies were omitted. All these control experiments indicate that most, if not all, staining observed in this study accounts for Parkin.

Regional distribution in the brain

Immunohistochemistry revealed a widespread expression of Parkin in many parts of the mouse brain (Fig. 3, Table 1). We have not observed differences in expression patterns among the different fixatives, nor between cryostate and paraffin sections or the various fixation procedures. Similarly, sections pre-incubated in Triton X-100 showed pronounced fibre staining, but no principal differences were noted.

Because the immunostainings detected with Rb1-/Rb2-antimsParkin1 and Rb3-antimsParkin2 differed only in intensity, results with these three antisera have been pooled and are presented together. Table 1 summarizes the distribution pattern in the adult mouse brain. A brief description of the results obtained in the different brain regions is given below.

Most immunoreactive cells were found in the hindbrain. Almost all the centres appeared distinctly positive for Parkin. Remarkably strong immunostaining was seen in all cranial nerve nuclei (Fig. 3D) and in the superior and inferior olive. The raphe nuclei, however, were free of Parkin staining.

In the cerebellum, cells within the cerebellar nuclei were positive, whereas the molecular and granular layer and the Purkinje cells were

FIG. 5. Electron micrographs of Parkin-immunopositive structures in the pontine nuclei (A and C), in the substantia nigra (B, D–F and H) and in the striatum (G and I). (A–C) Neurons with patchy distribution of labelling in the cytoplasma. The cell shown in (C) exhibits a speckled staining pattern in the nucleus. (D) Parkin-immunopositive microglial cell with reaction product in the cytoplasma and the nucleus. (E) Endothelial cell with Parkin immunoreactivity in the cytoplasma in the substantia nigra. (F) Perikaryal region of a neuron. Note, that the mitochondrial matrix (M) lacks reaction product. N, nucleus. (G–I) Synaptic contacts with Parkin staining. In G, the presynaptic terminal is heavily labelled. In H only the postsynaptic area is Parkin-immunopositive. Note the strong staining of the postsynaptic density. In I, both the pre- and postsynaptic areas show Parkin immunoreactivity. M, mitochondria. Arrows indicate synaptic clefts and stars indicate presynaptic terminals. Scale bars, 5 μm (A and B); 2 μm (C–E); and 0.5 μm (F–I).

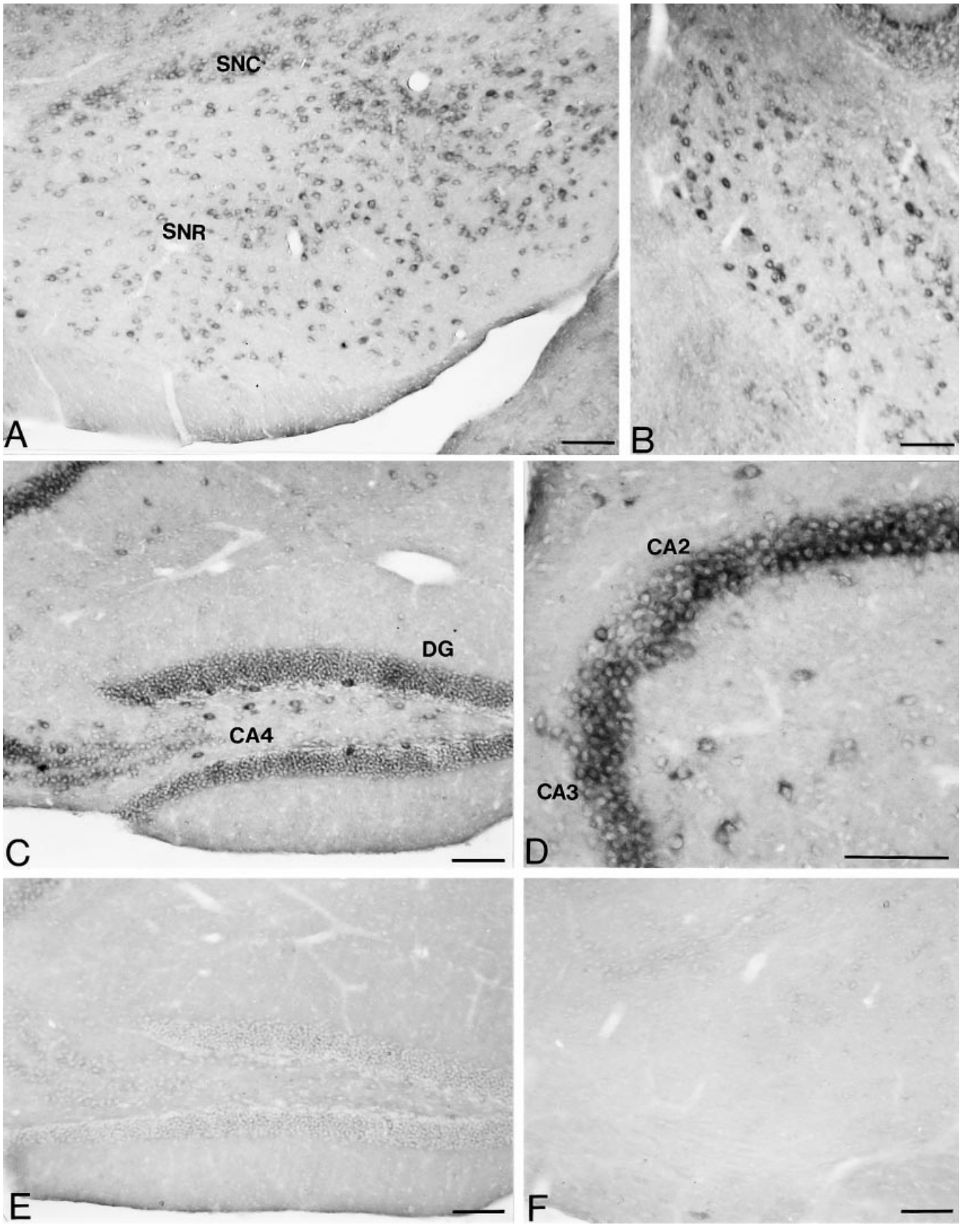
SNC
SNR
A
B
DG
CA4
C
CA2
CA3
D
E
F

negative. However, Parkin-immunopositive puncta were seen in close vicinity of Purkinje cells.

Structures located in the mesencephalon presented moderate to strong immunoreactivity. In the ventral part of the mesencephalon the red nucleus showed large, strongly stained cells. In the substantia nigra, moderate Parkin-immunopositive cells were confined to the pars reticulata (SNR) (Fig. 3E). In the dorsal mesencephalon, immunopositive cells were found in the intermediate and deep-grey layer of the superior colliculus and in all parts of the inferior colliculus.

In the diencephalon, the mammillary body, the zona incerta, the globus pallidus, the laterodorsal thalamic nucleus and the nucleus reticularis thalami displayed immunopositive cells.

In the hippocampal formation, the CA2 region showed the most remarkable staining pattern of the total brain (Fig. 3F). Precisely restricted to this area, the stratum oriens and stratum lacunosum moleculare displayed a strong punctate immunoreactivity. Moreover, many immunopositive spots delineated the pyramidal cells. Although few in number, strongly immunostained cells were also found in the hippocampus proper, and fascia dentata. They were seen in the stratum oriens and stratum lacunosum moleculare of CA1 and CA3, in the hilus and the granular layer of the fascia dentata. The molecular layer of the fascia dentata displayed a moderate neuropil staining.

Throughout the neocortex, single, immunoreactive, non-pyramidal neurons were detected. Significantly more Parkin-immunopositive cells were seen in the area 3 (somatosensory), where they were mainly concentrated in the deep layers V and VI. The retrosplenial cortex displayed a strong neuropil staining and a striking accumulation of Parkin-immunopositive cells in layer V (Fig. 3C). Moreover, Parkin-expressing cells were detected in the subiculum. In contrast, no Parkin-immunopositive cellular profiles were found in the striatum, but numerous immunopositive spots appeared in the neuropil (Fig. 3H).

The staining pattern seen in the Wistar rats appeared to be similar, if not identical, to that seen in the C57BL/6 mice. No staining was observed in human brain sections.

Cellular localization in the brain

In all brain regions examined, immunoprecipitate was largely limited to the soma and the proximal parts of cellular processes (Fig. 3I), both of which were stained in a granular fashion. Single cells in all brain regions examined exhibited immunoreactive spots scattered over the nucleus. The intensity of the immunoreaction was variable, depending on the area considered. Double immunofluorescence staining and sequential immunoperoxidase labelling of 4 μm-thick paraffin sections with the neuron-specific marker NeuN and Rb1-antimsParkin1 revealed that the majority of the cells were neurons (Fig. 4E and F). Comparison of adjacent paraffin sections, reactive for TH or ms Parkin, showed that the TH-immunoreactive cells in the ventral tegmental area and the SN pars compacta (SNC) do not express Parkin protein (Fig. 4A–D).

Ultrastructural analysis of sections immunolabelled with Rb1-antimsParkin1 confirmed the predominant neuronal localization and the patchy distribution pattern of Parkin protein (Fig. 5). In most neurons the reaction product was distributed in the cytoplasma of somata (Fig. 5A–C), in myelinated and unmyelinated axons, the reaction product was distributed in dendrites and also some presynaptic terminals (Fig. 5G and I). The latter was prominent in the striatum. It was found at the endoplasmic reticulum, the Golgi apparatus, the outer nuclear and mitochondrial membrane (Fig. 5F), and in postsynaptic densities (Fig. 5H and I). The matrix and the inner membrane of mitochondria were always devoid of immunostaining (Fig. 5F). Surprisingly, some neurons displayed clear patches of immunoreactivity in the nucleus (Fig. 5C). These nuclear patches were only found in neurons that exhibited cytoplasmic staining. The nuclear staining was independent from the fixative chosen.

Besides neurons, a small number of astrocytes, as well as endothelial and microglial cells showed punctate cytoplasmic or cytoplasmic and nuclear Parkin staining (Fig. 5D and E).

Parkin mRNA expression pattern

RT-PCR analysis revealed expression of Parkin in all brain areas investigated, i.e. whole brain, cerebral cortex, hippocampus, substantia nigra, cerebellum and brainstem (Fig. 2C). While the overall pattern of hybridization signal for both riboprobes was identical, the staining intensity differed between the two riboprobes. The hybridization signals with riboprobe 1 were generally weak, while those with riboprobe 2 were generally moderate to strong.

TABLE 2. Areas in the adult mouse brain which expressed Parkin mRNA

Telencephalon
Neocortex
Retrosplenial cortex
Hippocampus proper
Fascia dentata
Amygdaloid nuclei
Induseum griseum
Septum
Globus pallidus
Diencephalon
Laterodorsal thalamic nucleus
Mammillary body
Zona incerta
Mesencephalon
Superior colliculus
Inferior colliculus
Red nucleus
Substantia nigra (pars reticulata)
Substantia nigra (pars compacta)
Oculomotor nucleus (III)
Metencephalon
Medial cerebellar nucleus (fastigial)
Interposed cerebellar nucleus
Lateral cerebellar nucleus (dentate)
Cerebellar Purkinje cells
Myelencephalon
Pontine nuclei
Trigeminal nucleus (V)
Facial nucleus (VII)
Superior olive
Nuclei reticularis

FIG. 6. Parkin mRNA distribution in the adult mouse brain. Sections hybridized with antisense probe (riboprobe 2) show strong signal in the SN (A), dorsal cochlear nucleus (B) and hippocampus (C and D). Hybridization with the sense probe (riboprobe 2) resulted only in low background staining; hippocampus (E), SN (F). Abbreviations: CA2, hippocampal field CA2; CA3, hippocampal field CA3; CA4, hippocampal field CA4; DG, dentate gyrus; SNC, substantia nigra pars compacta; SNR, substantia nigra pars reticulata. Scale bars, 50 μm. brain region relative staining intensity.

Specificity of mRNA detection by ISH was determined by comparing the hybridization signals obtained with the different riboprobes. Since hybridization under identical conditions with a sense probe showed only background signals (Fig. 6E and F) and both riboprobes showed the same staining pattern, we concluded that the antisense signals were specific to Parkin mRNA. Moreover, ISH of COS cells transfected with mouse Parkin showed strong staining of single cells.

In agreement with the results obtained with immunohistochemistry, *in situ* hybridization revealed that the Parkin gene was widely expressed in the adult mouse CNS (Table 2). In general the distribution of Parkin mRNA appeared to be neuronal. A clear Parkin mRNA expression was observed in neurons of the SNR and SNC (Fig. 6A), the hippocampus (Fig. 6C and D), the cerebellar nuclei (Fig. 6B), the cerebral cortex, the facial and trigeminal nuclei, and the superior and inferior colliculus. In the hippocampus, mRNA-containing cells included the pyramidal cells in CA1–4, cells in the granule cell layer of the fascia dentata and single scattered cells in the stratum oriens and lacunosum moleculare of the hippocampus proper. The number of labelled cells in the cerebral cortex was high. In most cortical areas they distributed rather homogeneously over all layers, while in the retrosplenial cortex Parkin mRNA signal was strongest in layers IV and V. In the striatum no hybridization signal was seen.

Discussion

In our study we present a complete map of the distribution of Parkin protein and mRNA in the mouse CNS. This study also describes for the first time the ultrastructural localization of Parkin protein in neuronal and glial cells.

The principal findings of these studies are: (i) the widespread but heterogeneous distribution of Parkin in the mouse brain, (ii) the absence of Parkin protein in dopaminergic cells of the ventral tegmental area and substantia nigra pars compacta, (iii) the expression of Parkin in some endothelial and glial cells, and (iv) the speckled localization in single nuclei.

Regional distribution of Parkin

We demonstrate that Parkin is widely but non-homogeneously expressed in the mouse brain. The presence of Parkin (mRNA and protein) in all brain sub-regions is in agreement with previous reports in the human (Kitada *et al*., 1998; Solano *et al*., 2000) and rat brain (Horowitz *et al*., 1999). In most brain regions, a good correlation between the presence of protein and the presence of mRNA was observed. Nevertheless, exceptions were seen, particularly in the SNC, the hippocampus and the cerebellar Purkinje cells, where mRNA is found but no Parkin protein. Several reasons may account for this difference. The discrepancies could reflect masking of the antigen epitope by, say, a different conformation and/or interactions with other proteins or anterograde transport of the protein. The presumed function of Parkin as a carrier protein in the vesicular transport system (Shimura *et al*., 1999) and the presence of Parkin in nigrostriatal axons shown in our study and in that of the human brain (Shimura *et al*., 1999), support the latter hypothesis.

Although Parkin is found in all subdivisions of the brain the number of stained cells is clearly variable in the various brain regions. Low levels are found in the telencephalon and diencephalon, while in the brainstem a large number of heavily Parkin-immunopositive cells are detectable. The strongest staining was observed in the cranial nerve, pontine and cerebellar nuclei, the indusium griseum, the nuclei reticularis, as well as in the strata oriens and lacunosum moleculare of the hippocampal CA2 region. Since these areas are known to be involved in different brain functions, such as locomotion or emotion, memory and attention, and use different neurotransmitters, we conclude that Parkin is neither restricted to a single functional system nor associated with a particular transmitter phenotype. Double labelling studies are needed to confirm these observations.

The involvement of Parkin in the pathophysiology of the autosomal recessive juvenile and possibly also the sporadic form of parkinsonism (Hattori *et al*., 1998; Lücking *et al*., 1998; Tassin *et al*., 1998; Abbas *et al*., 1999; Nisipeanu *et al*., 1999; Satoh & Kuroda, 1999) anticipates the presence of Parkin in regions that are affected by Parkinson's disease, such as the SNC, the ventral tegmental area, the locus coeruleus, the dorsal raphe nucleus, parts of the oculomotor nucleus or some brainstem nuclei (Jellinger, 1991). Some of the areas affected in Parkinson's disease are strongly Parkin-immunopositive (e.g. the oculomotor nucleus) in the mouse brain, while others show only local axonal Parkin expression (e.g. the SNC) or even a lack of Parkin expression (e.g. the ventral tegmental area). Our ISH results in the SNC are in agreement with the reported presence of Parkin mRNA in human (Solano *et al*., 2000) and rat SNC (D'Agata *et al*., 2000). However, the immunostainings conflict with a study in the human brain, which demonstrated Parkin immunoreactivity in somata and processes of melanin-containing neurons of the SNC (Shimura *et al*., 1999) and a recent study in the rat brain, that describes a similarity between the topographic distribution of Parkin and dopaminergic neurons in the SNC (Horowitz *et al*., 1999). The lack of Parkin immunoreactivity in mouse dopaminergic somata of the SNC may reflect (i) masking of the epitope, (ii) anterograde transport of the protein, (iii) species differences in the expression of the protein, and/or (iv) differences in antibody specificity. On the other hand, the presence of Parkin protein in striatal terminals indicates (v) a local synthesis of Parkin in axon terminals. Recent studies are suggestive of extrasomatic *de novo* synthesis of proteins, most of which appear to be constituents of the slow axoplasmic transport rate groups (Van Minnen *et al*., 1997; Eng *et al*., 1999; Alvareza *et al*., 2000). The latter supports the hypothesis that Parkin plays a role as a carrier protein in transport systems (Shimura *et al*., 1999).

In contrast to our antiserum, the antibody (from Chemicon, CA, USA) used in the study of Horowitz *et al*. (1999) strongly labelled several bands in Western blot analysis, which were interpreted as post-translational modifications of the protein. Thus, it is conceivable that the positive staining of rat SNC is due to the presence of Parkin protein modifications that are not detected by our antiserum. The antibody from Chemicon showed no cross-reactivity to mouse Parkin in brain sections (data not shown).

Subcellular distribution of Parkin

This study has shown the presence of Parkin immunoreactivity, both in the cytoplasm and in the nucleus of a subset of neurons and in single glial cells. While only cells with a cytoplasmic staining revealed also nuclear immunoreactivity, the latter represent a subpopulation of Parkin-immunopositive cells.

The intense staining of cellular processes and somata suggests that Parkin is distributed throughout the entire neuron. Interestingly, the mitochondria lack immunostaining, which agrees with results of subcellular fractionation of human frontal lobe that show the majority of protein in the cytosol, but absence of protein in the mitochondrial fraction (Shimura *et al*., 1999). However, in contrast to the latter study, we observed Parkin protein in the nucleus. The appearance of the immunodeposits resembled the speckled compartment described by Leonhardt & Cardoso (1995), which is proposed to play a role in

pre-mRNA splicing. Within these speckled compartments, a number of small nuclear ribonucleoprotein particle (snRNP) components and non-snRNP splicing factors have been identified (Leonhardt & Cardoso, 1995). Most interesting, in this context, are analyses about the modular architecture of Parkin protein, which suggest a role in the regulation of gene expression. The first indications came from a study of Kitada and collaborators (1998). They showed that the C-terminal portion of Parkin contains a ring-finger motif, which may function as a zinc-finger protein in the regulation of gene expression. Subsequent studies discovered a ring-IBR (in between ring figure)-ring arrangement, which is used by proteins with DNA-binding and transcriptional activities (Morett & Bork, 1999). Interestingly, UCHL1 and α-synuclein, two other candidate proteins associated with familial cases of Parkinson's disease (Polymeropoulos *et al*., 1997; Leroy *et al*., 1998) were also found in the nucleus (Maroteaux *et al*., 1988; Wilson *et al*., 1988; Smith-Thomas *et al*., 1994; Nakajima *et al*., 1998; Kawashima *et al*., 2000; Masliah *et al*., 2000).

Although it is impossible to infer function merely from patterns of protein distribution, our morphological data suggest that Parkin protein is transported into processes but is also present in the nucleus and may therefore play a role in gene expression. Interestingly this pattern of subcellular distribution was also reported for the two other Parkinson-related proteins UCHL1 (Nakajima *et al*., 1998; Wilson *et al*., 1988; Smith-Thomas *et al*., 1994) and α-synuclein (Jensen *et al*., 1999; Kawashima *et al*., 2000; Masliah *et al*., 2000), for huntingtin (Block-Galarza *et al*., 1997; Dorsman *et al*., 1999) and for oestrogen receptors (Blaustein *et al*., 1992; Wagner *et al*., 1998). It will be of interest to see whether the extent and pattern of nuclear Parkin correlates with the physiological state of the cells.

Acknowledgements

We thank P. Jergolla, H. Schlierenkamp, M. Schneider and U. Hilsmann for excellent technical assistance.

Abbreviations

CA1, hippocampal field CA1; CA2, hippocampal field CA2; CA3, hippocampal field CA3; CPO, caudal periolivary nucleus; DG, dentate gyrus; IBR, in between ring figure; IMLF, interstitial nucleus of the medial longitudinal fasciculus; Int, interposed cerebellar nucleus; ISH, *in situ* hybridization; Lat, lateral cerebellar nucleus; LPGi, lateral paragigantocellular nucleus; LSO, lateral superior olive; Med, medial cerebellar nucleus; ML, medial mammillary nucleus, lateral part; PB, phosphate buffer; PBS, phosphate-buffered saline; PCRt, parvicellular reticular nucleus; PnC, pontine reticular nucleus; R, red nucleus; Rb1-antimsParkin1, antisera against mouse Parkin peptide 71–91 raised in rabbit 1; Rb2-antimsParkin1, antisera against mouse Parkin peptide 71–91 raised in rabbit 2; Rb3-antimsParkin2, antisera against mouse Parkin peptide 124–140 raised in rabbit 3; RT, room temperature; S, subiculum; SC, superior colliculus; SDS, sodium dodecyl sulphate; SNC, substantia nigra pars compacta; SNR, substantia nigra pars reticulata; TBS, Tris-buffered saline; TH, tyrosine hydroxylase; UCHL1, ubiquitin C-terminal hydrolase 1; VCP, ventral cochlear nucleus, posterior part; VTA, ventral tegmental area.

References

Abbas, N., Lücking, C.B., Ricard, S., Dürr, A., Bonifati, V., De Michele, G., Bouley, S., Vaughan, J.R., Gasser, T., Marconi, R., Broussolle, E., Brefel-Courbon, C., Harhangi, B.S., Oosrta, B.A., Fabrizio, E., Böhme, G.A., Pradier, L., Wood, N.W., Filla, A., Meco, G., Denefle, P., Agid, Y., Brice, A. & the French Parkinson's disease genetics study group, t.E.c.o.g.s.i.P.s.d. (1999) A wide variety of mutations in the Parkin gene are responsible for autosomal recessive Parkinsonism in Europe. *Hum. Mol. Gen.*, **8**, 567–574.

Alvareza, J., Giudittab, A. & Koenigc, E. (2000) Protein synthesis in axons and terminals: significance for maintenance, plasticity and regulation of phenotype. With a critique of slow transport theory. *Progr. Neurobiol.*, **62**, 1–62.

Blaustein, J.D., Lehman, M.N., Turcotte, J.C. & Greene, G. (1992) Estrogen receptors in dendrites and axon terminals in the guinea pig hypothalamus. *Endocrinology*, **131**, 281–290.

Block-Galarza, J., Chase, K.O., Sapp, E., Vaughn, K.T., Vallee, R.B., DiFiglia, M. & Aronin, N. (1997) Fast transport and retrograde movement of huntingtin and HAP 1 in axons. *Neuroreport*, **8**, 2247–2251.

D'Agata, V., Zhao, W. & Cavallaro, S. (2000) Cloning and distribution of the rat Parkin mRNA. *Mol. Brain Res.*, **75**, 345–349.

Dorsman, J.C., Smoor, M.A., Maat-Schieman, M.L., Bout, M., Siesling, S., van Duinen, S.G., Verschuuren, J.J., den Dunnen, J.T., Roos, R.A. & van Ommen, G.J. (1999) Analysis of the subcellular localization of huntingtin with a set of rabbit polyclonal antibodies in cultured mammalian cells of neuronal origin: comparison with the distribution of huntingtin in Huntington's disease autopsy brain. *Phil Trans R Soc. Lond B*, **354**, 1061–1067.

Eng, H., Lund, K. & Campenot, R.B. (1999) Synthesis of beta-tubulin, actin, and other proteins in axons of sympathetic neurons in compartemented cultures. Journal of. *Neuroscience*, **19**, 1–9.

Franklin, K.B.J. & Paxinos, G. (1997) *The Mouse Brain*. Academic Press, London.

Hattori, N., Matsumine, H., Asakawa, S., Kitada, T., Yoshino, H., Elibol, B., Brookes, A.J., Yamamura, Y., Kobayashi, T., Wang, M., Yoritaka, A., Minoshima, S., Shimizu, N. & Mizuno, Y. (1998) Point mutations (Thr240Arg and Ala311Stop) in the Parkin gene. *Biochem. Biophys. Res. Comm.*, **249**, 754–758.

Horowitz, J.M., Myers, J., Stachowiak, M.K. & Torres, G. (1999) Identification and distribution of Parkin in rat brain. *Neuroreport*, **10**, 3393–3397.

Jellinger, K.A. (1991) Pathology of Parkinson's disease. *Mol. Chem. Neuropathol.*, **14**, 153–197.

Jensen, P.H., Li, J.-Y., Dahlström, A. & Dotti, C.G. (1999) Axonal transport of synucleins is mediated by all rate components. *Eur. J. Neurosci.*, **11**, 3369–3376.

Kawashima, M., Suzuki, S.O., Doh-ura, K. & Iwaki, T. (2000) α-Synuclein is expressed in a variety of brain tumors showing neuronal differentiation. *Acta Neuropathol.*, **99**, 154–160.

Kitada, T., Asakawa, S., Hattori, N., Matsumine, H., Yamamura, Y., Minoshima, S., Yokochi, M., Mizuno, Y. & Shimizu, N. (1998) Mutations in the Parkin gene cause autosomal recessive juvenile Parkinsonism. *Nature*, **392**, 605–608.

Kitada, T., Asakawa, S., Minoshima, S., Mizuno, Y. & Shimizu, N. (2000) Molecular cloning, gene expression, and identification of a splicing variant of the mouse Parkin gene. *Mamm. Genome*, **11**, 417–421.

Leonhardt, H. & Cardoso, M.C. (1995) Targeting and association of proteins with functional domains in the nucleus. The insoluble solution. *Intl. Rev. Cytol.*, **162B**, 303–335.

Leroy, E., Boyer, R., Auburger, G., Leube, B., Ulm, G., Mezey, E., Harta, G., Brownstein, M.J., Jonnalagada, S., Chernova, T., Dehejia, A., Lavedan, C., Gasser, T., Steinbach, P.J., Wilkinson, K.D. & Polymeropoulos, M.H. (1998) The ubiquitin pathway. *Nature*, **395**, 451–452.

Lücking, C.B., Abbas, N., Dürr, A., Bonifati, V., Bonnet, A.-M., de Broucker, T., De Michele, G., Wood, N.W., Agid, Y., Brice, A. & for the European Consortium on Genetic Susceptibility in Parkinson's disease and The French Parkinson's disease genetics study group (1998) Homozygous deletions in Parkin gene in European and North African families with autosomal recessive juvenile Parkinsonism. *Lancet*, **352**, 1355–1356.

Maroteaux, L., Campanelli, J.T. & Scheller, R.H. (1988) Synuclein: a neuron-specific protein localized to the nucleus and presynaptic nerve terminal. *J. Neurosci.*, **8**, 2804–2815.

Masliah, E., Rockenstein, E., Veinbergs, I., Mallory, M., Hashimoto, M., Takeda, A., Sagara, Y., Sisk, A. & Mucke, L. (2000) Dopaminergic loss and inclusion body formation in alpha-synuclein mice. Implications for neurodegenerative disorders. *Science*, **287**, 1265–1269.

Matsumine, H., Saito, M., Shimoda-Matsubayashi, S., Tanaka, H., Ishikawa, A., Nakagawa-Hattori, Y., Yokochi, M., Kobayashi, T., Igarashi, S., Takano, H., Sanpei, K., Koike, R., Mori, H., Kondo, T., Mizutani, Y., Schäffer, A.A., Yamamura, Y., Nakamura, S., Kuzuhara, S., Tsuji, S. & Mizuno, Y. (1997) Localization of a gene for an autosomal recessive form of juvenile Parkinsonism to chromosome 6q25.2–27. *Am. J. Hum. Genet.*, **60**, 588–596.

McLean, I.W. & Nakane, P.K. (1974) Periodate-lysine-paraformaldehyde

fixative. A new fixation for immunoelectron microscopy. *J. Histochem. Cytochem.*, **22**, 1077–1083.
Morett, E. & Bork, P. (1999) A. novel transactivation domain in Parkin. *TIBS*, **24**, 229–231.
Nakajima, T., Murabayashi, C., Ogawa, K. & Taniguchi, K. (1998) Immunoreactivity of protein gene product 9.5 (PGP 9.5) in the developing hamster olfactory bulb. *Anat. Rec.*, **250**, 238–244.
Neuhoff, V.P.K., Zimmer, H.G. & Mesecke, S. (1979) A simple and vertsatile, sensitive and volume -independent method for quantitative protein determination with independence of other external influences. *Hoppe-Seyler's Z. Physiol. Chem.*, **360**, 1657–1670.
Nisipeanu, P., Inzelberg, R., Blumen, S.C., Carasso, R.L., Hattori, N., Matsumine, H. & Mizuno, Y. (1999) Autosomal-recessive juvenile Parkinsonism in a Jewish Yemenite kindred. mutation of Parkin gene. *Neurology*, **53**, 1602–1604.
Paxinos, G. & Watson, C. (1998) *The Rat Brain*. Academic Press, San Diego, CA.
Polymeropoulos, M.H., Lavedan, C., Leroy, E., Ide, S.E., Dehejia, A., Dutra, A., Pike, B., Root, H., Rubenstein, J., Boyer, R., Stenroos, E.S., Chandrasekharappa, S., Athanassiadou, A., Papapetropoulos, T., Johnson, W.G., Lazzarini, A.M., Duvoisin, R.C., Di Iorio, G., Golbe, L.I. & Nussbaum, R.L. (1997) Mutation in the α-synuclein gene identified in families with Parkinson's disease. *Science*, **276**, 2045–2047.
Satoh, J. & Kuroda, Y. (1999) Association of codon 167 Ser/Asn heterozygosity in the Parkin gene with sporadic Parkinson's disease. *Neuroreport*, **10**, 2735–2739.
Shimura, H., Hattori, N., Kubo, S., Yoshikawa, M., Kitada, T., Matsumine, H., Asakawa, S., Minoshima, S., Yamamura, Y., Shimizu, N. & Mizuno, Y. (1999) Immunohistochemical and subcellular localization of Parkin protein. absence of protein in autosomal recessive juvenile Parkinsonism patients. *Ann. Neurol.*, **45**, 668–672.
Smith-Thomas, L.C., Kent, C., Mayer, R.J. & Scotting, P.J. (1994) Protein ubiquination and neuronal differentiation in chick embryos. *Dev. Brain Res.*, **81**, 171–177.
Solano, S.M., Miller, D.W., Augood, S.J., Young, A.B. & Penney, J.B. (2000) Expression of alpha-synuclein, Parkin, and ubiquitin carboxy-terminal hydrolase L1 mRNA in human brain. genes associated with familial Parkinson's disease. *Ann. Neurol.*, **47**, 201–210.
Stichel, C.C., Singer, W. & Zilles, K. (1990) Ultrastructure of PkC (II/III)-immunopositive structures in rat primary visual cortex. *Exp. Brain Res.*, **82**, 575–584.
Tassin, J., Dürr, A., de Broucker, T., Abbas, N., Bonifati, V., De Michele, G., Bonnet, A.-M., Broussolle, E., Pollak, P., Vidailhet, M., De Mari, M., Marconi, R., Medjbeur, S., Filla, A., Meco, G., Agid, Y., Brice, A. & the French Parkinson's disease genetics study group, T.E.C.O.G.S.i.P.S.d. (1998) Chromosome 6-linked autosomal recessive early-onset Parkinsonism: linkage in European and algerian families, extension of the clinical spectrum and evidence of a small homozygous deletion in one family. *Am. J. Hum. Genet.*, **63**, 88–94.
Van Minnen, J., Bergman, J.J., Van Kesteren, E.R., Smit, A.B., Geraerts, W.P., Lukowiak, K., Hasan, S.U. & Syed, N.I. (1997) De novo protein synthesis in isolated axons of identified neurons. *Neurosci.*, **80**, 1–7.
Wagner, V.C.K., Silverman, A.J. & Morrell, J.I. (1998) Evidence for estrogen receptor in cell nuclei and axon terminals within the lateral habenula of the rat. regulation during pregnancy. *J. Comp. Neurol.*, **392**, 330–342.
Wahle, P. (1994) Combining non-radioactive in situ hybridization with immunohistological and anatomical techniques. In Wisden, W. (eds), *In Situ Hybridization Protocols for the Brain.* Academic Press, London, UK, pp. 98–120.
Wilson, P.O.G., Barber, P.C., Hamid, Q.A., Power, B.F., Dhillon, A.P., Rode, J., Day, I.N.M., Thompson, R.J. & Polak, J.M. (1988) The immunolocalization of protein gene product 9.5 using rabbit polyclonal and mouse monoclonal antibodies. *Br. J. Exp. Pathol.*, **69**, 91–104.